Article

Language-led Visual Grounding for Human Computer Interaction

Zezhou Sui [1,‡], Mian Zhou [1,‡*], Zhikun Feng[1], Angelos Stefanidis[2] and Nan Jiang[3]

[1] School of Computer Science and Engineering, Tianjin University of Technology, Tianjin 300384, China
[2] School of AI and Advanced ComputingXi'an Jiaotong-Liverpool University, Taicang, Suzhou, Jiangsu 215412, China ; Angelos.Stefanidis@xjtlu.edu.cn
[3] Department in Computing and Informatics, Bournemouth University, Poole, BH12 5BB, UK; njiang@bournemouth.ac.uk
* Correspondence: zhoumian@tjut.edu.cn; Tel.: +86-022-60216865
‡ These authors contributed equally to this work.

Abstract: In recent years, with the rapid development of computer vision technology and the popularization of intelligent hardware, as well as people's increasing demand for intelligent products for human-computer interaction, visual grounding technology can help machines and humans identify and locate objects, thereby promoting human-computer interaction and intelligent manufacturing. At the same time, human-computer interaction is constantly evolving and improving, becoming increasingly intelligent, humane, and efficient. This paper proposes a new VG model and designs a language verification module that uses language information as the main information to increase the model's interactivity. Additionally, we propose the combination of visual grounding and human-computer interaction, aiming to explore the research status and development trends of visual grounding and human-computer interaction technology, as well as their application in practical scenarios and optimization directions, to provide references and guidance for relevant researchers and promote the development and application of visual grounding and human-computer interaction technology.

Keywords: visual grounding; human-computer interaction; intelligent systems; user experience; interaction design

1. Introduction

Human-Computer Interaction (HCI) has evolved significantly over the years, transforming the way we interact with technology. One of the key challenges in HCI is bridging the gap between human perception and the machine's understanding of the visual world. Visual grounding, a fundamental concept in computer vision, has emerged as a crucial approach to address this challenge. In this article, we will explore the concept of visual grounding and its applications in HCI, highlighting its potential to enhance our interactions with computers and devices.

One key emerging technology in computer vision[1,2] is Visual Grounding (VG), which refers to the process of establishing a correspondence between visual information and its associated meaning in the real world. It enables computers to recognize and interpret objects, actions, and scenes depicted in images or videos, facilitating meaningful interactions with users. By grounding visual information, computers can understand and respond to user queries, instructions, and gestures, opening up new possibilities for natural and intuitive interfaces. These technologies have many applications, including image retrieval[3], robot localization[4], image captioning[5], and so on. On the other hand, HCI technology focuses on developing interfaces that allow humans to interact with computers in a natural and intuitive way. This technology includes various modes such as voice, gesture, touch, and eye-tracking. These modes can be used alone or in combination to provide seamless and intuitive interaction between humans and computers.

Preprints (www.preprints.org) | NOT PEER-REVIEWED | Posted: 13 June 2023 doi:10.20944/preprints202306.0959.v1

In this article, we present a novel VG method within the context of HCI. Our work contributes in three main aspects:

- Proposal of the new model: We introduce a new model in the VG field that effectively processes visual and language features in a symmetric manner. This symmetric processing can better understand semantic information and improve the overall performance of VG systems. Additionally, we design a language-driven, multi-stage cross-modal decoder in the decoder section to iteratively locate targets based on language information, thereby increasing the model's interactivity;
- Experimental Validation: We conducted extensive experiments to evaluate the efficacy of our proposed method. Through these experiments, we demonstrate the advantages and improvements achieved by our model on several well-established benchmarks[6–8] in the field of VG;
- Linking between VG and HCI: In addition to the empirical validation, we propose a connection between visual grounding and human-computer interaction. By highlighting the synergies between these two fields, we propose feasible future applications of VG within the domain of HCI. These applications encompass various aspects around HCI, offering new possibilities for enhanced user experiences and intuitive interactions.

The structure of the paper is as follows. In Section 2, we will elaborate on previous work on VG, including the methods used. In Section 3, we introduce our model and the methods used in it. In Section 4, we will introduce configuration, settings, and dataset used in our model experiments, the experimental setup, and the results obtained. In Section 5, we will discuss the connection between VG and HCI, as well as some potential future application scenarios.

2. The previous development in Visual Grounding

Existing VG methods can be divided into three categories: Two-stage methods[6,7,9,10], One-stage methods[11–13] and End-to-end Transformer-based methods[14,15]. Both one-stage and two-stage methods treat VG as a ranking problem of detected candidate regions. One-stage methods[11–13,16] directly embed text and fuse image features to generate dense predictions, from which the one with the highest confidence is selected. Two-stage methods[10,17–24] first generate a set of object proposals and then match them with language queries to retrieve top-ranked proposals. Both methods rely on pre-detected proposals or predefined anchor box configurations for inference, and they match or fuse candidate objects with text embeddings based on region features (corresponding to predicted proposals) or point features (corresponding to dense anchor boxes). However, such feature representations may not be flexible enough to capture detailed visual concepts or context mentioned in language descriptions[14].

Although convolutional neural networks (CNNs) have achieved excellent performance in various visual tasks[25–30], the success of transformers in the fields of vision and language has attracted attention in the research community. Transformers have replaced CNNs in many visual tasks, such as image classification[2] and object detection[1,31]. The success of transformers in these areas has also driven the transformation of VG. In recent Transformer-based methods, such as TransVG[14,15], a ResNet+Transformer encoder and BERT are used in the backbone to extract visual and language features respectively. The two features are projected into the same dimension using a linear projection layer, and a simple stack of Transformer encoder blocks is used in the fusion stage to merge them. The output of the fusion module is directly fed into an MLP to generate the four-dimensional coordinates of the localized object. This approach achieves higher accuracy than one-stage and two-stage methods on most datasets. However, the problem with TransVG[15] is that the fusion stage uses a simple stack of Transformer encoder blocks, which, although effective, is too simple, resulting in suboptimal experimental accuracy. VLTVG[14] solves the problem of overly simple fusion in the fusion stage. It introduces a multi-stage cross-modal decoder with query as the query, which calculates and outputs discriminative

Preprints (www.preprints.org) | NOT PEER-REVIEWED | Posted: 13 June 2023 doi:10.20944/preprints202306.0959.v1

features based on the validation score input by the visual-language verification module and the visual context feature and visual feature output by the language-guided context module. These features are then passed together with the language features into the multi-stage cross-modal decoder, and the final output after the last layer of features is fed into an FFN layer to generate the four-dimensional coordinates of the located object. VLTVG solves the problem of simple stacking of Transformer encoder blocks in TransVG[15], but the model mainly processes visual features and neglects language feature processing, leading to a lack of semantic understanding of language features in the entire model. There are also other approaches that use transformers or attention mechanisms to tackle various types of vision and language tasks[32–35]. For instance, SCAN[33] addresses image-text matching by modeling correlations when proposing candidate bounding boxes. STVGBert[35] associates text embeddings with video frame features for video grounding. In contrast, we focus more on image-based grounding, using pixel-level modeling of visual-language correlations.

3. Language-led Visual Grounding Method

In this section, we will mainly introduce our proposed model. We will firstly present the overall structure of the model. Then we elaborate each module used in the model, including the verification module, context encoder module, and multi-stage cross-modal decoder module.

3.1. The framework: a model of encoder to decoder

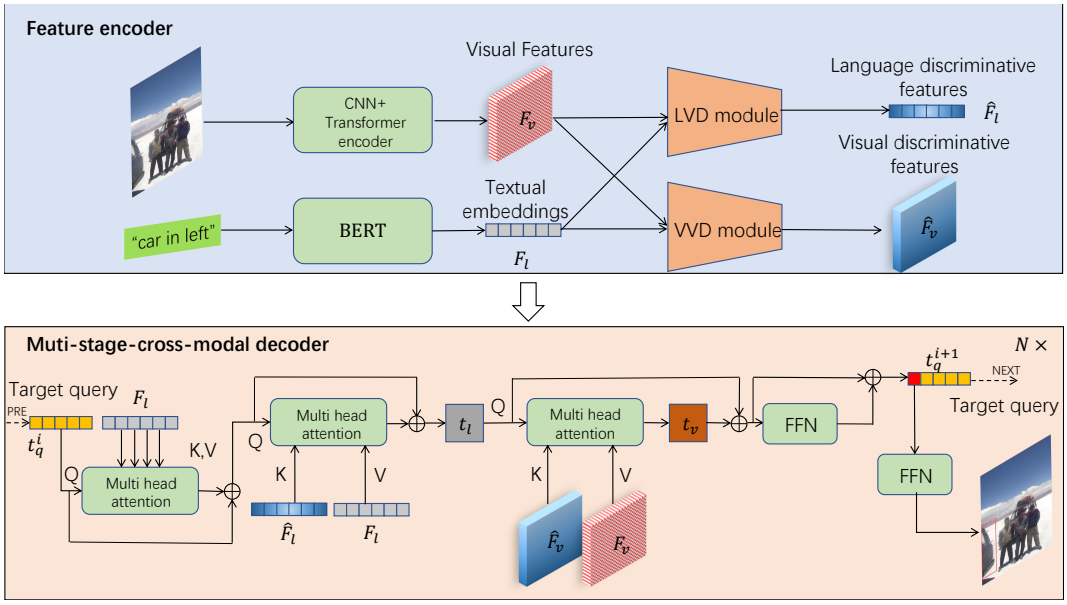

Figure 1. The overall encoder and decoder architecture of our proposed model is constructed as follows. Given the input image and language expression, the Feature Encoder first extracts visual features and textual embeddings separately. Then, the LVD module (Language Verification Discriminative module) and VVD module (Visual Verification Discriminative module) are used to process the features to generate discriminative features corresponding to the language and visual features, respectively. Finally, the multi-stage cross-modal decoder is utilized to iteratively infer the target location using all the generated visual and language features. The normalization layer and normalization layer are not indicated in the figure.

Our proposed model follows the same approach as previous transformer-based models in directly locating objects based on their features. As shown in Figure 1, given an input image and language sentence, we first extract features separately by feeding images and sentences into two independent branches respectively. For the image, we use a stack of transformer encoder layers on top of ResNet50[25] to generate the 2D feature map $F_v \in \mathbb{R}^{C\times H\times W}$. For the language sentence, we use BERT[36] to encode it into a textual embedding

Preprints (www.preprints.org) | NOT PEER-REVIEWED | Posted: 13 June 2023 doi:10.20944/preprints202306.0959.v1

sequence $F_l \in \mathbb{R}^{C\times L}$. Based on these two modalities, we use the Visual Verification Discriminative (VVD) module and the Language Verification Discriminative (LVD) module to encode them into discriminative features. In the VVD module, we employ a visual-linguistic verification module and a language-guided contextual module to encode the referenced features. In the LVD module, we use similar operations to those in the VVD module, but instead we validate the language features based on visual features, allowing the language features to focus more on the parts of visual information that are relevant to the language sentence. Finally, we apply a multi-stage cross-modal decoder to iteratively attend to the visual and language feature information encoded by the encoders for more accurate retrieval of object representations for object localization.

3.2. Language Verification Discriminative (LVD) Module

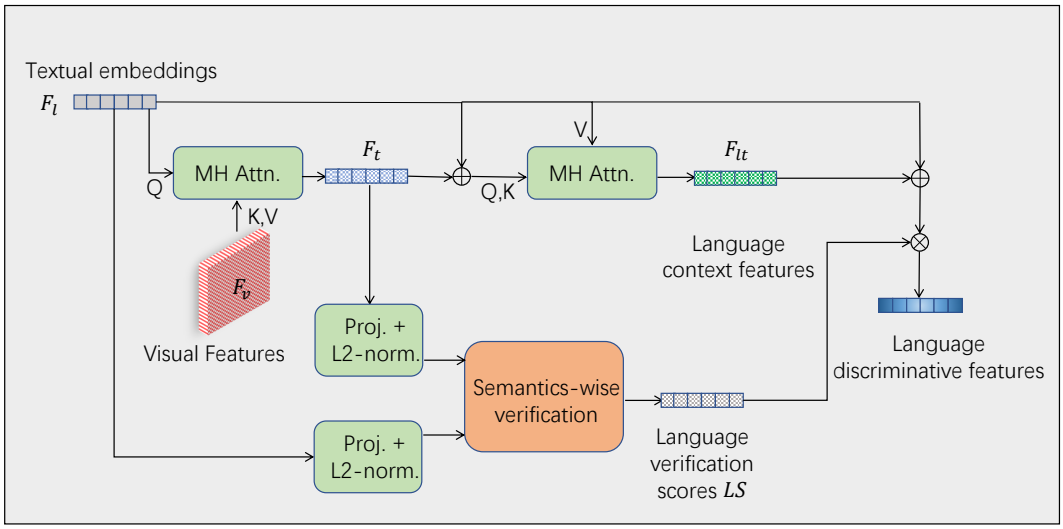

Figure 2. The Language Verification Discriminative Module (LVD) is based on multi-head attention, which uses multiple attention heads to capture visual information and model the correlation between visual information and language expression, ultimately outputting language discriminative features.The normalization layer and normalization layer are not indicated in the figure.

The input language sentence is encoded by BERT into the feature F_l, which only contains semantic understanding, but not any visual prior knowledge. Without the prior knowledge, solely using language features to index object instances in images may lead to incorrect indexing or eventually failure to locate the object finally. Therefore, it is necessary to integrate visual features into the module.The language verification discriminative module (LVD) integrates visual information into the language features by computing language discriminative features.

The Language Verification Discriminative Module in Figure 2 is based on multi-head attention[37]. It uses the language feature $F_l \in \mathbb{R}^{C\times L}$ as a query, and the visual feature $F_v \in \mathbb{R}^{C\times H\times W}$ as keys and values. Through multi-head attention, relevant visual semantic information is collected for the language feature reference, resulting in F_t, which is the language representation corresponding to visual features. Then, F_l' and F_t' are projected onto the same semantic space through a projection layer and L2-norm layer, and their semantic correlation score LS is calculated as the verification score for each spatial position (x, y):

$$LS(x,y) = \alpha \cdot \exp\left(-\frac{\left(1 - F_l'(x,y)^T F_t'(x,y)\right)^2}{2\sigma^2}\right) \tag{1}$$

where, α and σ are learn-able parameters. The verification score represents the semantic correlation score between the visual feature and the corresponding language semantic feature. For each language feature, the verification score models the correlation based

Preprints (www.preprints.org) | NOT PEER-REVIEWED | Posted: 13 June 2023 doi:10.20944/preprints202306.0959.v1

on visual feature. When the visual features are multiplied with the language feature, the features we obtained will naturally suppress some stimulation which is irrelevant to visual information. However, while modeling the correlation between language features and visual features, the location information or other relevant information in the language representation may be suppressed also. It would lead to incomplete understanding of the language representation by the model. Therefore, the language features should also have visual contextual information, such as interactive relationships and positional relationships. It combines the position and other information in the language representation with visual features, enabling the model to better understand information from the language extent. This is also crucial for modeling the objects or other parts in images.

As the second Multi-head Attention of Figure 2, F_t is added to F_l, and the sum as query and key. F_l serves as value for multi-head attention to obtain F_{lt}. The information in F_{lt} represents the visual semantic information collected from visual features through multi-head attention and the language contextual features obtained from the interaction between visual features and language features. The attention formula is as follows:

$$\begin{cases} Q = W_Q^T(F_l + F_t) \\ K = W_k^T(F_l + F_t) \\ \text{attn}_{i,j} = \text{softmax}\left(\frac{Q(i)^T\left(K(j) + W_K^T R(i-j)\right)}{\sqrt{d_k}}\right) \end{cases} \tag{2}$$

where W_Q and W_K are the projection weights for query and key, d_k is the dimension of the projection channel, and $R(\cdot)$ is the sine positional encoding for relative position[37]. Finally, we combine the language verification score LS with F_{lt} to obtain the language discrimination feature $\widehat{F}_l$:

$$\widehat{F}_l = (F_l + F_{lt}) \cdot LS \tag{3}$$

The language verification discriminative feature $\widehat{F}_l$ will be applied in the final multi-stage cross-modal decoder.

3.3. Visual Verification Discriminative (VVD) Module

In the VVD module, we employ a visual-linguistic verification module and a language-guided contextual module to encode the referenced features. The visual-linguistic verification module refines the visual features to focus on those that are relevant to the language sentence. The language-guided contextual module collects information-rich visual contextual information to aid in object recognition.

The input image is first encoded by a convolution neural network and then encoded into visual feature map F_v by Transformer encoder layers. This feature map contains the features of object instances in the image, but no prior knowledge of the language description. Retrieval without any prior knowledge is likely to be distracted by the features of other object instances or regions, leading to inaccurate localization.Therefore, the Visual Language Verification module allows the injection of language information into visual features, enabling the visual features to possess rich language prior knowledge. As shown in Figure 3, the Visual-Linguistic Verification Module (VLVM) is based on multi-head attention. The visual feature map $F_v \in \mathbb{R}^{C\times H\times W}$ is used as the query and the textual embedding $F_l \in \mathbb{R}^{C\times L}$ is used as the key and value. Though multi-head attention, relevant semantic information is collected for some visual feature. Then, the projected feature maps F_v' and F_s' are obtained by projection and L2-norm layers into the same semantic space. Their semantic correlation score is calculated as the verification score for each spatial location (x, y)

$$S(x,y) = \alpha \cdot \exp\left(-\frac{\left(1 - F_v'(x,y)^T F_s'(x,y)\right)^2}{2\sigma^2}\right) \tag{4}$$

where α and σ are learn-able parameters as well. These verification score measures the correlation between each visual feature and the textual embedding. When the embedding

Preprints (www.preprints.org) | NOT PEER-REVIEWED | Posted: 13 June 2023 doi:10.20944/preprints202306.0959.v1

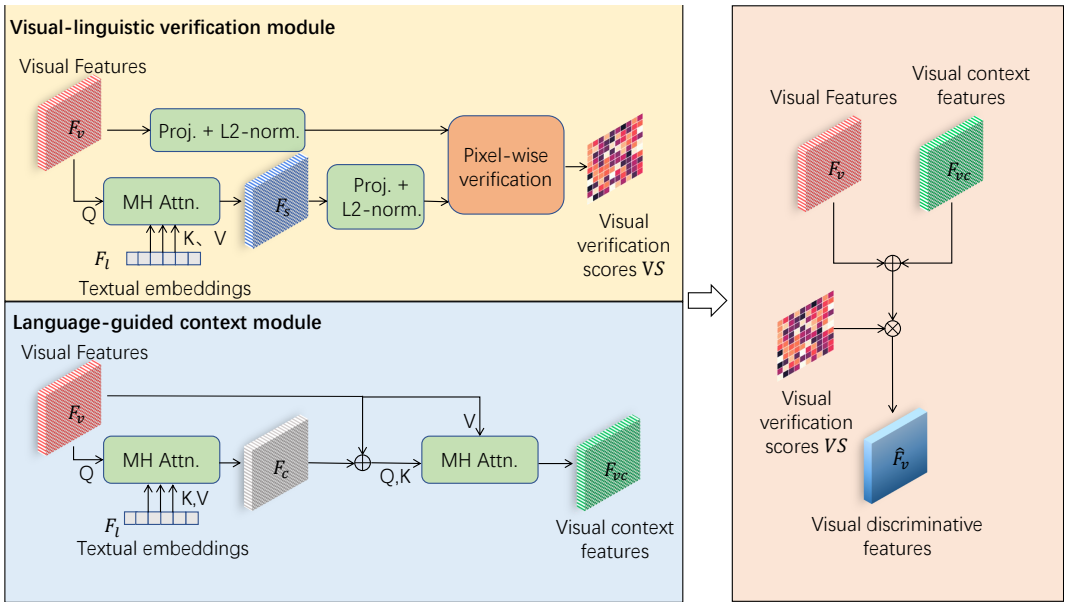

Figure 3. Visual Verification Discriminative Module (VVD). The VVD module is also based on multi-head attention and consists of two sub-modules: visual-linguistic verification module and language-guided context module. The visual-linguistic verification module models the correlation between language information and visual information pixel-by-pixel through multi-head attention to obtain visual verification scores. The language-guided context module uses multi-head attention to obtain contextual information of language features and obtain visual context features. Finally, the visual verification scores, visual context features, and visual features are combined to calculate the visual discriminative features.

multiplied with the visual feature, the resulting feature naturally suppresses the textual parts that are irrelevant.

While using the VLD module to model the correlation, the visual features should also contain visual context, such as interactive relationships and positional relationships, which are crucial for modeling the target object and other parts.The Language-Guided Context module effectively combines the interaction, location, and other information about objects in the language expression with visual features, forming visual features with contextual information. As shown in Figure 3, the language-guided context module is also based on Multi-Head Attention. F_v is used as the query, and F_l is used as the key and value to obtain F_c, which contains semantic information and is the corresponding language representation of the visual features. Then, F_c is added with F_v as the query and key, and F_v is used as the value for again to obtain the visual context feature F_{vc}, which contains the visual representation of the contextual information in the language description. The attention formula for F_{vc} is as follows:

$$\begin{cases} Q = W_Q^T(F_v + F_c) \\ K = W_k^T(F_v + F_c) \\ \text{attn}_{i,j} = \text{softmax}\left(\frac{Q(i)^T\left(K(j)+W_K^T R(i-j)\right)}{\sqrt{d_k}}\right) \end{cases} \tag{5}$$

where W_Q and W_K are the projecting weights for query and key, d_k is the dimension of the projecting channel, and $R(\cdot)$ is the sine encoding of relative position. To establish more discriminative features for the target object, we use the same approach to fuse the contextual features F_{vc} and the visual verification scores S with the visual features F_v:

$$\widehat{F_v} = (F_v + F_{vc}) \cdot S \tag{6}$$

Preprints (www.preprints.org) | NOT PEER-REVIEWED | Posted: 13 June 2023 doi:10.20944/preprints202306.0959.v1

The generated visual discriminative feature $\widehat{F}_v$ is also applied in the final multi-stage cross-modal decoder.

3.4. Multi-stage-cross-modal Decoder

We use a multi-stage cross-modal decoder that takes language features as queries to perform the final object localization task by leveraging the established visual feature map and text embedding. The decoder can repeatedly process visual and language information, thereby distinguishing the target object from other objects.

In Figure 1, we illustrate the architecture of the multi-stage cross-modal decoder that we use language features as queries to perform final target localization task with the established visual feature maps and text embedding. The decoder is composed of N stages, each of which consists of the same network architecture (weights are not shared) for iterative cross-modal reasoning. In the first stage, we use a learn-able target query $t_q^1 \in \mathbb{R}^{c \times x}$ as the initial representation of the target object, where x is set to 5. The target query is fed into the decoder to extract visual features based on the language expression and update its feature representation to $t_q^i (1 \leq i \leq N)$ at the beginning of each subsequent stage. The feature updating process for each decoder is shown in Figure 1. Specifically, in the i-th stage, the target query t_q^i is used as a query and fed into the first multi-head attention module, where language features are used as keys and values for multi-head attention, aiming to imbue the target query with language information that can query the relevant parts in both language and visual information encoded by the text embedding. After obtaining the language information, it is fed into the second multi-head attention module, where the previously computed language discrimination feature $\widehat{F}_l$ is used as keys and the language feature F_l is used as values for multi-head attention to compute the relevance with the previous language discrimination feature, resulting in $t_l \in \mathbb{R}^{c \times 5}$, which contains the semantic information of the language expression corresponding to the visual part of interest. Then, in the third multi-head attention module, we use t_l as the query, $\widehat{F}_v$ as the keys, and F_v as the values to compute the relevance with the previous visual discrimination feature and collect the interested part from the visual feature map F_v based on the semantic description collected in t_l, generating the collected visual feature $t_v \in \mathbb{R}^{c \times 5}$ for the referenced object. Finally, t_v is used to update the target query t_q^i:

$$\begin{cases} t_q' = LN\left(t_q^i + t_v\right) \\ t_q^{i+1} = LN\left(t_q' + FFN\left(t_q'\right)\right) \end{cases} \tag{7}$$

where, $LN(\cdot)$ stands for layer normalization, and $FFN(\cdot)$ is a feed-forward neural network consisting of two linear projection layers with ReLU activation layer. The updated t_q^{i+1} is then fed into the next level decoder for iterative cross-modal inference and feature representation updates.

We used five target queries to represent the target object, but only the first target query was used for prediction and back-propagation updates during the final prediction process. This way, other interfering information is concentrated in the last four target queries, making it simple and efficient, and eliminating the need to use a classification head to detect whether the feature representation in the target query is a representation of the query object. Based on this multi-level decoder, using target queries can focus on different descriptions of the referring expressions, enabling us to collect more complete features of the target objects. Furthermore, we can use the collected features to further refine and improve the target queries t_q^i, forming a more accurate representation of the target objects. Finally, we predict the bounding box of the referenced object by attaching a three-layer MLP with ReLU activation function to the output of each stage's target query, and supervise all predicted bounding boxes equally to facilitate multi-level decoder training.

Preprints (www.preprints.org) | NOT PEER-REVIEWED | Posted: 13 June 2023 doi:10.20944/preprints202306.0959.v1

4. Experiments

In this section, we firstly talk about how to implement the proposed methods, and display the results secondly.

4.1. Implementation Detail

We set the size of the input image to 640×640 and the maximum length of the language expression to 40. During inference, we dynamically adjust the size of the input image according to the input image, so that the longer edge equals 640 and the shorter edge is padded to 640. At the beginning and end of the language expression, we added [CLS] and [SEP] tokens respectively, and then processed them using BERT[36]. We perform data augmentation during training, following previous work[12,13,15,16].

In the visual feature extraction branch, we use ResNet50 as our CNN backbone, followed by 6 transformer encoder layers of the visual feature extraction branch, which we initialize using the corresponding weights of the DETR model [1]. In the text embedding extraction branch, we initialize the corresponding weights using BERT[36]. During the training process, we used AdamW optimizer[38] to train our model, with a batch size of 8. We trained for a total of 90 epochs, and in the first 10 epochs, we froze the weights of the feature extraction branch (i.e., the CNN+transformer encoder layers and BERT). This allowed our model to train more stably. We set the initial learning rate of the network to 10^{-4}, the initial learning rate of the feature extraction layers to 10^{-5}, and decay the learning rate by a factor of 10 after 60 epochs of training. We use the same loss function as previously used in Transformer-based methods. Since our network directly regresses to the coordinates of bounding boxes, we avoid positive/negative sample assignment and can directly use the predicted bounding boxes to calculate the loss:

$$L = \sum_{i=1}^{N} \lambda_{\text{giou}} L_{\text{giou}} \left(b, \hat{b}^i\right) + \lambda_{L1} L_{L1}\left(b, \hat{b}^i\right) \tag{8}$$

where, b represents the ground-truth bounding box, and $\left\{\hat{b}^i\right\}_{i=1}^{N}$ represents the predicted bounding boxes from stage 1 to stage N. λ_{giou} and λ_{L1} denote the GIoU loss[39] and L1 loss, respectively, and λ_{giou} and λ_{L1} are hyper-parameters that balance the two losses, which are set to 2 and 5, respectively.

We follow the evaluation metrics used in previous works[15,16]. Given an image and a language expression, a predicted bounding box is considered correct if its Intersection over Union (IoU) with the ground truth bounding box is greater than 0.5.

4.2. Results

In Table1, we report the performance comparison of our method with other state-of-the-art methods on three popular benchmark visual localization datasets: RefCOCO[6], RefCOCO+[6], and RefCOCOg[7].Our method outperforms other methods in some of the datasets. Table2 also shows the performance of our method on the test set of ReferItGame[8]. Our method is significantly better than one-stage and two-stage methods and also leads in Transformer-based methods. As ReferIGame dataset is annotated through refer it game, which has strong interactivity in data format and annotation, the performance comparison on ReferIGame dataset indicates that our model is superior to other methods in terms of interaction.

Preprints (www.preprints.org) | NOT PEER-REVIEWED | Posted: 13 June 2023 doi:10.20944/preprints202306.0959.v1

Table 1. Comparison of our method with other state-of-the-art methods on RefCOCO[6], RefCOCO+[6], and RefCOCOg[7].For the data not given in the model paper, we use "-" instead.

Models	Venue	BackBone	RefCOCO			RefCOCO+			RefCOCOg		
			val	testA	testB	val	testA	testB	val-g	val-u	test-u
Two-stage Models											
CMN[18]	*CVPR'17*	VGG16	-	71.03	65.77	-	54.32	47.76	57.47	-	-
VC[23]	*CVPR'18*	VGG16	-	73.33	67.44	-	58.40	53.18	62.30	-	-
ParalAttn[24]	*CVPR'18*	VGG16	-	75.31	65.52	-	61.34	50.86	58.03	-	-
MAttNet[22]	*CVPR'18*	ResNet-101	76.65	81.14	69.99	65.33	71.62	56.02	-	66.58	67.27
LGRANs[20]	*CVPR'19*	VGG16	-	76.60	66.40	-	64.00	53.40	61.78	-	-
DGA[21]	*ICCV'19*	VGG16	-	78.42	65.53	-	69.07	51.99	-	-	63.28
RvG-Tree[17]	*TPAMI'19*	ResNet-101	75.06	78.61	69.85	63.51	67.45	56.66	-	66.95	66.51
NMTree[19]	*ICCV'19*	ResNet-101	76.41	81.21	70.09	66.46	72.02	57.52	64.62	65.87	66.44
Ref-NMS[40]	*AAAI'21*	ResNet-101	80.70	84.00	76.04	68.25	73.68	59.42	-	70.55	70.62
One-stage Models											
SSG[11]	*arXiv'18*	DarkNet-53	-	76.51	67.50	-	62.14	49.27	47.47	58.80	-
FAOA[13]	*ICCV'19*	DarkNet-53	72.54	74.35	68.50	56.81	60.23	49.60	56.12	61.33	60.36
RCCF[12]	*CVPR'20*	DLA-34	-	81.06	71.85	-	70.35	56.32	-	-	65.73
ReSC-Large[16]	*ECCV'20*	DarkNet-53	77.63	80.45	72.30	63.59	68.36	56.81	63.12	67.30	67.20
LBYL-Net[41]	*CVPR'21*	DarkNet-53	79.67	82.91	74.15	68.64	73.38	59.49	62.70	-	-
Transformer-based Models											
TransVG[15]	*ICCV'21*	ResNet-50	80.32	82.67	78.12	63.50	68.15	55.63	66.56	67.66	67.44
TransVG[15]	*ICCV'21*	ResNet-101	81.02	82.72	78.35	64.82	70.70	56.94	67.02	68.67	67.73
ours		ResNet-50	**84.00**	**87.64**	**79.31**	**72.67**	**78.17**	**63.51**	**71.71**	**74.63**	**73.36**

Table 2. Comparison with the state-of-the-art methods on the test sets of ReferItGame[8].

Models	BackBone	ReferItGame test
Two-stage Models		
CMN[18]	VGG16	28.33
VC[23]	VGG16	31.13
MAttNet[22]	ResNet-101	29.04
Similarity Net[10]	ResNet-101	34.54
CITE[42]	ResNet-101	35.07
DDPN[43]	ResNet-101	63.00
One-stage Models		
SSG[11]	DarkNet-53	54.24
ZSGNet[44]	ResNet-50	58.63
FAOA[13]	DarkNet-53	60.67
RCCF[12]	DLA-34	63.79
ReSC-Large[16]	DarkNet-53	64.60
LBYL-Net[41]	DarkNet-53	67.47
Transformer-based Models		
TransVG[15]	ResNet-50	69.76
TransVG[15]	ResNet-101	70.73
VLTVG[14]	ResNet-50	71.60
VLTVG[14]	ResNet-101	71.84
ours	ResNet-50	**72.45**

Figure 4 showcases the output results of our model, revealing a high degree of accuracy in the majority of the localization outcomes. The predicted results of our model closely match the ground truths, indicating its proficiency in localizing objects within images. However, we also present instances of localization failures in Figure 4, accompanying the language expressions associated with the respective images. In these particular examples, the model tends to mislocate the objects, potentially due to a limited understanding of the language expressions relevant to the given image. As a result, the model heavily relies on

Preprints (www.preprints.org) | NOT PEER-REVIEWED | Posted: 13 June 2023 doi:10.20944/preprints202306.0959.v1

Figure 4. The comparison between our model's localization results and the ground truth bounding boxes is shown. The green boxes represent the ground truths, while the red boxes indicate the predicted bounding boxes by our model. Additionally, we present three examples of localization errors, with the language expressions associated with the erroneous examples marked with an asterisk (*).

Preprints (www.preprints.org) | NOT PEER-REVIEWED | Posted: 13 June 2023 doi:10.20944/preprints202306.0959.v1

visual cues alone for localization, leading to inaccuracies. For example, in the second-to-last image in Figure4, the requested localization phrase is "girl with mic," but the model's localization result does not match the ground truth. Instead, it localizes to the girl on the left. This could be due to the model not encountering the term "mic" during training, leading to a lack of understanding of the complete meaning of the language expression and resulting in localization to the most prominent girl.

5. VG applications in HCI

VG is an inherently interconnected field with HCI. The purpose of this paper is to delve into the present research landscape and emerging trends concerning VG and HCI techniques. It also aims to identify application scenarios and optimization directions for practical implementation. Here are potential applications applied to HCI in the future.

5.1. Image Dataset Annotation

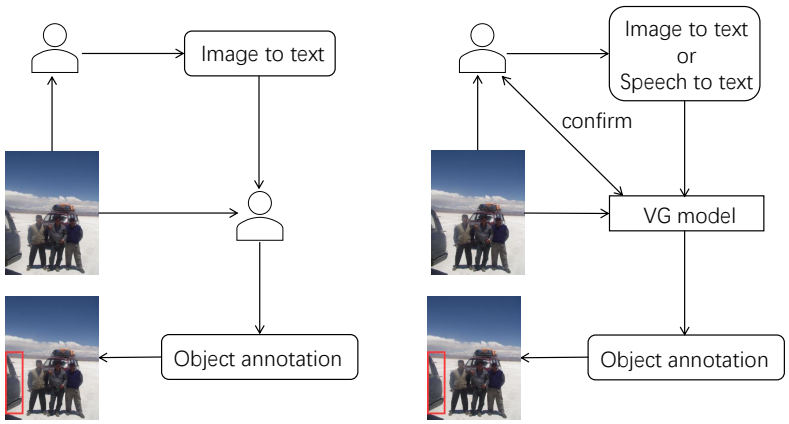

(a) Traditional methods for annotating datasets (b) Improved method using VG model

Figure 5. The previous dataset annotation process and the process of dataset annotation using VG technology are shown in the flowchart. Figure (a) represents the previous dataset annotation process, while Figure (b) represents the process of dataset annotation using VG technology.

There is a growing trend towards the utilization of larger visual and multimodal models in recent times. However, training these models on large datasets necessitates a significant amount of data to facilitate effective learning of the given task. Unfortunately, the process of annotating image data is both laborious and costly. One potential solution to address this challenge is to integrate VG as a fundamental component with other algorithms, thereby creating an automatic image dataset annotation tool. As shown in Figure 5(a), traditional dataset annotation consists of two main parts. Firstly, a dataset organiser/manager generate describes the objects to be annotated in the images in terms of language expressions. Then, workers annotate/label the objects in the images according to the language expressions. This purely manually approach naturally brings with serveral major problems. Firstly, it requires hiring a large amount of personnel to annotate the data, when the dataset become large. Secondly, there is no specific standard for workers to manually annotate data, the position and size of objects are annotated at workers' will. it leads to inconsistency when different workers have different annotation style. In deep learning, the high-quality of annotation in a dataset is crucial for accurate classification, detection, and segmentation, while an inconsistent dataset degrades the performance of deep learning systems. Lastly, employing humans to perform such repetitive and tedious tasks is not in line with the principles of Human-Computer Interaction (HCI).

Preprints (www.preprints.org) | NOT PEER-REVIEWED | Posted: 13 June 2023 doi:10.20944/preprints202306.0959.v1

To address the limitations of traditional data annotation methods mentioned above, we have made improvements by incorporating VG technology as a replacement for extensive manual operations. We present a process flow diagram illustrating the data annotation procedure using VG technology, as shown in Figure 5(b). Our approach also consists of two main parts: the generation of language expressions as the first step, localization annotation using VG technology serves as the second step. The first step involves manually describing the objects that need to be annotated to generate language expressions. We only rely on human input in this step because the selection and description of language expressions are subjective tasks that are challenging for current technology to replace with automated processes. When generating language expressions, there are two options for input: direct text input and voice input using devices with language recognition capabilities. After generating the language expressions, we feed the images and language expressions into our VG model to perform object localization annotation. In this step, we utilize VG technology to replace manual annotation because it involves repetitive labeling tasks that do not require strong subjectivity. Additionally, using machines for annotation leads to faster processing, ensures consistent labeling style, and improves the overall quality of the dataset.

After the model completes the annotation process, we interact with the user to verify the accuracy of the annotations. If the annotations fail, we either reposition and re-annotate them or ask the organiser to provide a more precise language expression for the model to perform the repositioning and annotation.

5.2. Interactive Object Tracking

VG can be integrated with other technologies to enable real-time object detection and tracking, which has numerous applications in human-computer interaction (HCI). For example, cameras can use this technology to track people or robots. In the paradigm of tracking by learning, when tracking pedestrians in a crowded scene, initial object detectors may present multiple objects as tracking candidates at the start of tracking. A human operator may then select an object of interest to track. However, it can be challenging for the human operator to communicate to the computer which object to track, and it may even be impossible to switch to a different object during the tracking process. Furthermore, there is currently no provision for interactive operations during target selection.

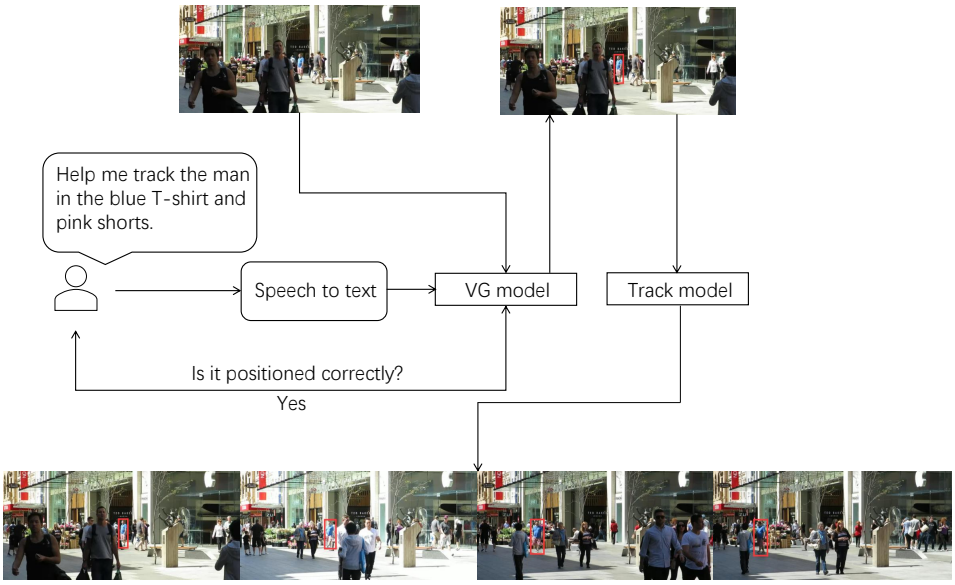

Figure 6. Interactive Object Tracking Process Diagram. The images in the diagram represent different frames of a video to illustrate the tracking process.

We propose an interactive object tracking system to overcome the limitations of traditional object tracking approaches. As illustrated in Figure 6, when a human operator

 doi:10.20944/preprints202306.0959.v1

encounters a scene with multiple pedestrians and decides on a target to track, an oral instruction is released by the operator and transformed into text using a Speech-to-Text module, such as a voice recognition device. The first frame image and the language expression are then input into a VG model for target localization. Once the VG model completes the localization, the operator is asked to verify whether it is correct. If the localization is not correct, the system will either re-localize or wait for the operator to provide a more accurate target description until the localization is correct. Once the target localization is completed, the VG-based results and the remaining video frames are fed into a tracking model. The tracking model utilizes the VG localization results to track the target in the subsequent video frames.

The interactive object tracking system we have designed is highly adaptable and can be used in various work environments. For instance, if the tracking task involves recognizing a single object, the system can easily be adapted by replacing the input expression with a specific expression for that object. This flexibility allows the system to be customized for different tracking tasks and makes it more versatile and widely applicable.

6. Conclusions

Visual Grounding (VG) is a rapidly growing area of research that seeks to bridge the gap between human perception and machine comprehension. It holds great promise for revolutionizing the way we interact with computers and devices, leading to significant advancements in Human-Computer Interaction (HCI). In this article, we focus on a specific aspect of VG, namely the integration of computer vision and natural language into HCI. By combining these two fields, we have explored the possibilities for future developments and applications. As these advancements continue, we can expect to see more natural, intuitive, and immersive interactions between humans and computers, ultimately enhancing our daily lives and experiences.

Although VG has made significant advancements, there are still several challenges that need to be addressed. Some of the key challenges include dealing with ambiguity, incorporating temporal information for dynamic scenes, and achieving robustness to changes in lighting, viewpoints, or occlusions. Additionally, ethical considerations, such as privacy, bias, and fairness, must be carefully addressed when deploying VG technologies in Human-Computer Interaction (HCI). To promote responsible and inclusive HCI, it is essential to ensure transparency, accountability, and user consent. Handling these challenges will be critical in realizing the full potential of VG and ensuring that it benefits society as a whole.

Author Contributions: Conceptualization, Zezhou Sui and Mian Zhou; methodology, Zezhou Sui; software, Zezhou Sui; validation, Zezhou Sui and Mian Zhou; formal analysis, Zezhou Sui; investigation, Nan Jiang; resources, Angelos Stefanidis; data curation, Zhikun Feng; writing—original draft preparation, Zezhou Sui; writing—review and editing, Mian Zhou; visualization, Zezhou Sui.; supervision, Mian Zhou; project administration, Mian Zhou; funding acquisition, Mian Zhou. All authors have read and agreed to the published version of the manuscript.

Funding: This research was funded by National Natural Science Foundation of China (61872270).

Institutional Review Board Statement: Not applicable.

Informed Consent Statement: Not applicable.

Data Availability Statement: An implementation is available at https://github.com/fest007/LVVVG.

Acknowledgments: In this section you can acknowledge any support given which is not covered by the author contribution or funding sections. This may include administrative and technical support, or donations in kind (e.g., materials used for experiments).

Conflicts of Interest: The authors declare no conflict of interest.

Abbreviations

The following abbreviations are used in this manuscript:

VG	Visual Grounding
HCI	Human Computer Interaction
CNN	Convolution Neural Network
LD	Linear dichroism

References

1. Carion, N.; Massa, F.; Synnaeve, G.; Usunier, N.; Kirillov, A.; Zagoruyko, S. End-to-end object detection with transformers. In Proceedings of the Computer Vision–ECCV 2020: 16th European Conference, Glasgow, UK, August 23–28, 2020, Proceedings, Part I 16. Springer, 2020, pp. 213–229.
2. Dosovitskiy, A.; Beyer, L.; Kolesnikov, A.; Weissenborn, D.; Zhai, X.; Unterthiner, T.; Dehghani, M.; Minderer, M.; Heigold, G.; Gelly, S.; et al. An image is worth 16x16 words: Transformers for image recognition at scale. *arXiv preprint arXiv:2010.11929* **2020**.
3. Datta, R.; Joshi, D.; Li, J.; Wang, J.Z. Image retrieval: Ideas, influences, and trends of the new age. *ACM Computing Surveys (Csur)* **2008**, *40*, 1–60.
4. Betke, M.; Gurvits, L. Mobile robot localization using landmarks. *IEEE transactions on robotics and automation* **1997**, *13*, 251–263.
5. You, Q.; Jin, H.; Wang, Z.; Fang, C.; Luo, J. Image captioning with semantic attention. In Proceedings of the Proceedings of the IEEE conference on computer vision and pattern recognition, 2016, pp. 4651–4659.
6. Yu, L.; Poirson, P.; Yang, S.; Berg, A.C.; Berg, T.L. Modeling context in referring expressions. In Proceedings of the Computer Vision–ECCV 2016: 14th European Conference, Amsterdam, The Netherlands, October 11-14, 2016, Proceedings, Part II 14. Springer, 2016, pp. 69–85.
7. Mao, J.; Huang, J.; Toshev, A.; Camburu, O.; Yuille, A.L.; Murphy, K. Generation and Comprehension of Unambiguous Object Descriptions. In Proceedings of the Proceedings of the IEEE Conference on Computer Vision and Pattern Recognition (CVPR), June 2016.
8. Kazemzadeh, S.; Ordonez, V.; Matten, M.; Berg, T. Referitgame: Referring to objects in photographs of natural scenes. In Proceedings of the Proceedings of the 2014 conference on empirical methods in natural language processing (EMNLP), 2014, pp. 787–798.
9. Nagaraja, V.K.; Morariu, V.I.; Davis, L.S. Modeling Context Between Objects for Referring Expression Understanding. In Proceedings of the Computer Vision – ECCV 2016; Leibe, B.; Matas, J.; Sebe, N.; Welling, M., Eds., Cham, 2016; pp. 792–807.
10. Wang, L.; Li, Y.; Huang, J.; Lazebnik, S. Learning Two-Branch Neural Networks for Image-Text Matching Tasks. *IEEE Transactions on Pattern Analysis and Machine Intelligence* **2019**, *41*, 394–407. https://doi.org/10.1109/TPAMI.2018.2797921.
11. Chen, X.; Ma, L.; Chen, J.; Jie, Z.; Liu, W.; Luo, J. Real-time referring expression comprehension by single-stage grounding network. *arXiv preprint arXiv:1812.03426* **2018**.
12. Liao, Y.; Liu, S.; Li, G.; Wang, F.; Chen, Y.; Qian, C.; Li, B. A real-time cross-modality correlation filtering method for referring expression comprehension. In Proceedings of the Proceedings of the IEEE/CVF Conference on Computer Vision and Pattern Recognition, 2020, pp. 10880–10889.
13. Yang, Z.; Gong, B.; Wang, L.; Huang, W.; Yu, D.; Luo, J. A fast and accurate one-stage approach to visual grounding. In Proceedings of the Proceedings of the IEEE/CVF International Conference on Computer Vision, 2019, pp. 4683–4693.
14. Yang, L.; Xu, Y.; Yuan, C.; Liu, W.; Li, B.; Hu, W. Improving visual grounding with visual-linguistic verification and iterative reasoning. In Proceedings of the Proceedings of the IEEE/CVF Conference on Computer Vision and Pattern Recognition, 2022, pp. 9499–9508.
15. Deng, J.; Yang, Z.; Chen, T.; Zhou, W.; Li, H. Transvg: End-to-end visual grounding with transformers. In Proceedings of the Proceedings of the IEEE/CVF International Conference on Computer Vision, 2021, pp. 1769–1779.
16. Yang, Z.; Chen, T.; Wang, L.; Luo, J. Improving one-stage visual grounding by recursive sub-query construction. In Proceedings of the Computer Vision–ECCV 2020: 16th European Conference, Glasgow, UK, August 23–28, 2020, Proceedings, Part XIV 16. Springer, 2020, pp. 387–404.
17. Hong, R.; Liu, D.; Mo, X.; He, X.; Zhang, H. Learning to compose and reason with language tree structures for visual grounding. *IEEE transactions on pattern analysis and machine intelligence* **2019**, *44*, 684–696.
18. Hu, R.; Rohrbach, M.; Andreas, J.; Darrell, T.; Saenko, K. Modeling relationships in referential expressions with compositional modular networks. In Proceedings of the Proceedings of the IEEE conference on computer vision and pattern recognition, 2017, pp. 1115–1124.
19. Liu, D.; Zhang, H.; Wu, F.; Zha, Z.J. Learning to assemble neural module tree networks for visual grounding. In Proceedings of the Proceedings of the IEEE/CVF International Conference on Computer Vision, 2019, pp. 4673–4682.
20. Wang, P.; Wu, Q.; Cao, J.; Shen, C.; Gao, L.; Hengel, A.v.d. Neighbourhood watch: Referring expression comprehension via language-guided graph attention networks. In Proceedings of the Proceedings of the IEEE/CVF Conference on Computer Vision and Pattern Recognition, 2019, pp. 1960–1968.
21. Yang, S.; Li, G.; Yu, Y. Dynamic graph attention for referring expression comprehension. In Proceedings of the Proceedings of the IEEE/CVF International Conference on Computer Vision, 2019, pp. 4644–4653.

22. Yu, L.; Lin, Z.; Shen, X.; Yang, J.; Lu, X.; Bansal, M.; Berg, T.L. Mattnet: Modular attention network for referring expression comprehension. In Proceedings of the Proceedings of the IEEE conference on computer vision and pattern recognition, 2018, pp. 1307–1315.
23. Zhang, H.; Niu, Y.; Chang, S.F. Grounding referring expressions in images by variational context. In Proceedings of the Proceedings of the IEEE Conference on Computer Vision and Pattern Recognition, 2018, pp. 4158–4166.
24. Zhuang, B.; Wu, Q.; Shen, C.; Reid, I.; Van Den Hengel, A. Parallel attention: A unified framework for visual object discovery through dialogs and queries. In Proceedings of the Proceedings of the IEEE Conference on Computer Vision and Pattern Recognition, 2018, pp. 4252–4261.
25. He, K.; Zhang, X.; Ren, S.; Sun, J. Deep residual learning for image recognition. In Proceedings of the Proceedings of the IEEE conference on computer vision and pattern recognition, 2016, pp. 770–778.
26. Ren, S.; He, K.; Girshick, R.; Sun, J. Faster r-cnn: Towards real-time object detection with region proposal networks. *Advances in neural information processing systems* **2015**, *28*.
27. Xu, Y.; Huang, Z.; Lin, K.Y.; Zhu, X.; Shi, J.; Bao, H.; Zhang, G.; Li, H. Selfvoxelo: Self-supervised lidar odometry with voxel-based deep neural networks. In Proceedings of the Conference on Robot Learning. PMLR, 2021, pp. 115–125.
28. Xu, Y.; Lin, J.; Shi, J.; Zhang, G.; Wang, X.; Li, H. Robust self-supervised lidar odometry via representative structure discovery and 3d inherent error modeling. *IEEE Robotics and Automation Letters* **2022**, *7*, 1651–1658.
29. Xu, Y.; Lin, K.Y.; Zhang, G.; Wang, X.; Li, H. RNNPose: Recurrent 6-DoF object pose refinement with robust correspondence field estimation and pose optimization. In Proceedings of the Proceedings of the IEEE/CVF Conference on Computer Vision and Pattern Recognition, 2022, pp. 14880–14890.
30. Xu, Y.; Zhu, X.; Shi, J.; Zhang, G.; Bao, H.; Li, H. Depth completion from sparse lidar data with depth-normal constraints. In Proceedings of the Proceedings of the IEEE/CVF International Conference on Computer Vision, 2019, pp. 2811–2820.
31. Zhu, X.; Su, W.; Lu, L.; Li, B.; Wang, X.; Dai, J. Deformable detr: Deformable transformers for end-to-end object detection. *arXiv preprint arXiv:2010.04159* **2020**.
32. Chen, Y.; Gong, S.; Bazzani, L. Image search with text feedback by visiolinguistic attention learning. In Proceedings of the Proceedings of the IEEE/CVF Conference on Computer Vision and Pattern Recognition, 2020, pp. 3001–3011.
33. Lee, K.H.; Chen, X.; Hua, G.; Hu, H.; He, X. Stacked cross attention for image-text matching. In Proceedings of the Proceedings of the European conference on computer vision (ECCV), 2018, pp. 201–216.
34. Lu, J.; Batra, D.; Parikh, D.; Lee, S. Vilbert: Pretraining task-agnostic visiolinguistic representations for vision-and-language tasks. *Advances in neural information processing systems* **2019**, *32*.
35. Su, R.; Yu, Q.; Xu, D. Stvgbert: A visual-linguistic transformer based framework for spatio-temporal video grounding. In Proceedings of the Proceedings of the IEEE/CVF International Conference on Computer Vision, 2021, pp. 1533–1542.
36. Devlin, J.; Chang, M.W.; Lee, K.; Toutanova, K. Bert: Pre-training of deep bidirectional transformers for language understanding. *arXiv preprint arXiv:1810.04805* **2018**.
37. Vaswani, A.; Shazeer, N.; Parmar, N.; Uszkoreit, J.; Jones, L.; Gomez, A.N.; Kaiser, Ł.; Polosukhin, I. Attention is all you need. *Advances in neural information processing systems* **2017**, *30*.
38. Loshchilov, I.; Hutter, F. Decoupled weight decay regularization. *arXiv preprint arXiv:1711.05101* **2017**.
39. Rezatofighi, H.; Tsoi, N.; Gwak, J.; Sadeghian, A.; Reid, I.; Savarese, S. Generalized intersection over union: A metric and a loss for bounding box regression. In Proceedings of the Proceedings of the IEEE/CVF conference on computer vision and pattern recognition, 2019, pp. 658–666.
40. Chen, L.; Ma, W.; Xiao, J.; Zhang, H.; Chang, S.F. Ref-nms: Breaking proposal bottlenecks in two-stage referring expression grounding. In Proceedings of the Proceedings of the AAAI conference on artificial intelligence, 2021, Vol. 35, pp. 1036–1044.
41. Huang, B.; Lian, D.; Luo, W.; Gao, S. Look before you leap: Learning landmark features for one-stage visual grounding. In Proceedings of the Proceedings of the IEEE/CVF Conference on Computer Vision and Pattern Recognition, 2021, pp. 16888–16897.
42. Plummer, B.A.; Kordas, P.; Kiapour, M.H.; Zheng, S.; Piramuthu, R.; Lazebnik, S. Conditional image-text embedding networks. In Proceedings of the Proceedings of the European Conference on Computer Vision (ECCV), 2018, pp. 249–264.
43. Yu, Z.; Yu, J.; Xiang, C.; Zhao, Z.; Tian, Q.; Tao, D. Rethinking diversified and discriminative proposal generation for visual grounding. *arXiv preprint arXiv:1805.03508* **2018**.
44. Sadhu, A.; Chen, K.; Nevatia, R. Zero-shot grounding of objects from natural language queries. In Proceedings of the Proceedings of the IEEE/CVF International Conference on Computer Vision, 2019, pp. 4694–4703.